Materials Physics and Mechanics. 2023;51(6): 76-83
Research article
http://dx.doi.org/10.18149/MPM.5162023_7

Submitted: October 5, 2023
Approved: November 3, 2023
Accepted: November 14, 2023

# Disclination models in the analysis of stored energy in icosahedral small particles

**A.L. Kolesnikova [1,2] ✉, M.V. Dorogov [2], S.A. Krasnitckii [1,2], A.M. Smirnov [2], A.E. Romanov [2]**

[1] Institute for Problems of Mechanical Engineering RAS, St. Petersburg, Russian Federation

[2] ITMO University, St. Petersburg, Russian Federation

✉ anna.kolesnikova.physics@gmail.com

**Abstract.** A discrete disclination model that describes the stored energy in icosahedral small particles (ISPs) is proposed. The particle energy is defined as a superposition of the energies of six interacting wedge disclinations, each of which connects the opposite vertices of the icosahedron. Isotropic elasticity analytical solution is given for a spheroid with the volume being equal to that of the icosahedron. Distributed disclination model, also known as Marks-Ioffe model, is used for calculation of the stored in ISP energy. The influence of the Poisson's ratio on the stored in ISP energy is studied within both considered disclination models.
**Keywords:** disclination; icosahedral small particle; discrete disclination model; distributed disclination model

***Acknowledgements.*** *The work was supported by the Russian Science Foundation (grant No 19-19-00617).*

**Citation:** Kolesnikova AL, Dorogov MV, Krasnitckii SA, Smirnov AM, Romanov AE. Disclination models in the analysis of stored energy in icosahedral small particles. *Materials Physics and Mechanics*. 2023;51(6): 76-83. DOI: 10.18149/MPM.5162023_7.

## Introduction

The interest to pentagonal crystals did increase after Dan Shechtman discovery of quasicrystals in the mid-1980s [1,2], for which he was awarded by Nobel Prize in chemistry in 2011. Being different from quasicrystals in the type of atomic ordering, icosahedral small particles (ISPs) share with the first ones a remarkable feature of having habitus with five-fold symmetry [3]. It was first proposed [4,5] and then supported by experimental data [6,7] that a ISP consists of twenty crystalline domains with FCC crystal structure interconnected by coherent twin boundaries. Such multiple cyclic twinning induces inhomogeneous elastic deformation in particle interior, which can be described in terms of wedge disclinations [8]. These structural features largely determine the unique functional properties of ISPs. In particular, it is precisely with the presence of twin boundaries and residual deformations that the higher chemical activity of ISPs is associated having the same size as for cubic or octahedral shape monocrystalline ones [9–11]. In addition, specific pentagonal shape of particles contributes to an increase in the intensity of plasmon resonance peaks, and can also leads to their splitting [12,13].

It should be noted that despite the active research of many unique nanomaterials over the past 20 years, only a small part has reached the large-scale applied use in various household and specialized devices of electronics and optoelectronics. The reason for this is not so much the

high cost and complexity of producing nanomaterials, but the significant uncontrolled effect of crystal structure defects on the functional properties of nanomaterials [14–16]. This highlights the great impact of theoretical studies of the defect structure of ISPs, too.

The distributed disclination model [17], also known as Marks-Ioffe model, for the analysis of intrinsic elastic strain in ISPs has been usually employed to provide a theoretical description of the relaxation phenomena in such microparticles. According to this model, the ISP is treated as an elastic sphere with the residual strain caused by removing the solid angle 0.0613 with subsequent recovering of the continuity. Theoretical studies [18] have shown that the distributed disclination model makes it possible to find the elastic fields and energy of ISPs, expressed in simple for analysis analytical equations. On the other hand, the behavioral features of the ISPs, such as the growth of a pentagonal crystalline whisker from the apex of the ISP [19–21], can only be explained by discrete disclination model. The residual elastic strain in the discrete model is induced by six wedge disclinations with strength ~ 7.333° crossing the particle through the opposite icosahedron vertices [7,22]. This representation is able to describe the inhomogeneous residual strains in ISPs to precise the results of existing theoretical models of stress relaxation as well as to create new models taking into consideration the defect formation in vicinity of disclination lines.

Even though the discrete model of ISPs was proposed more than twenty years ago, some of its aspects require clarification, in particular, ISP nonuniform elastic filed and stored energy associated with this field, which are the purpose of this work.

**Discrete disclination model**

A pentagonal microcrystal with a habitus of regular icosahedron contains six positive wedge disclinations penetrating the crystal and passing through its center (Fig. 1(a)) [7,22]. The outcrops of the disclination lines on the surface coincide with the vertices of the icosahedron. The plane angles between the disclination lines $\alpha$ are all the same and equal to 63.435°:

$$\alpha = \arccos\left(\frac{2R_{cs}^2 - g_{ih}^2}{2R_{cs}^2}\right) = \arccos\left(\frac{1}{\sqrt{5}}\right) \approx 63.435°, \quad (1)$$

where $R_{cs}$ is circumscribed sphere radius, $R_{cs} = \sqrt{2(5+\sqrt{5})}g_{ih}/4$; $g_{ih}$ is icosahedron edge.

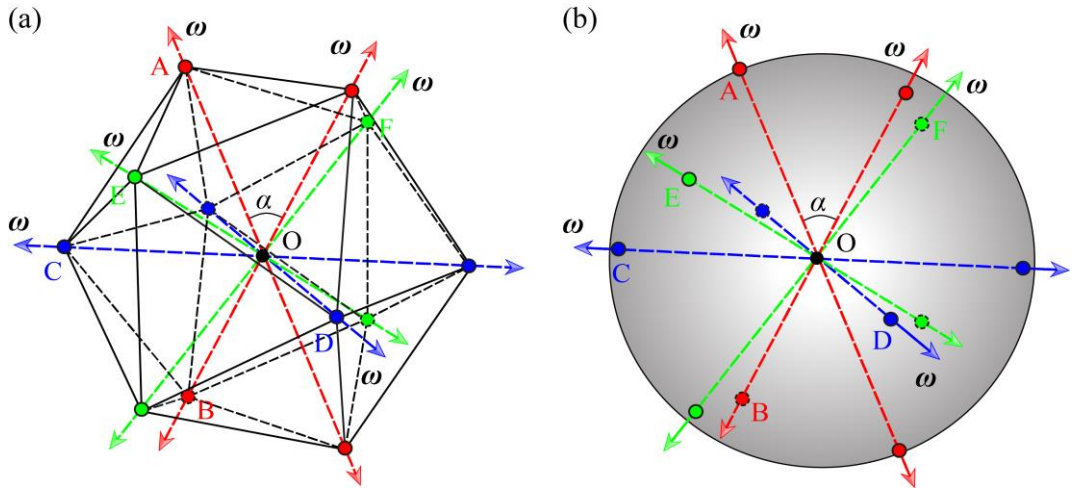


**Fig. 1.** Schematics of icosahedral small particle (a) and its discrete disclination model (b). A, B, C, D, E, and F are wedge disclinations in the particle interior; O is the center of the icosahedron and the point of the intersection of disclination lines; $\boldsymbol{\omega}$ is Frank pseudovector; $\alpha$ is the flat angle between disclinations. The invisible edges of the icosahedron are indicated by black dashed lines. Disclination lines are shown by colored dashed lines

As a simplified discrete model of such an ISP, we adopted an elastic sphere with six positive disclinations with strength $\omega \approx 7.333°$ passing through its center [23,24] (Fig. 1(b)). The disclinations are positioned in the sphere in the same way as they are positioned in the ISP shown in Fig. 1(a).

In the framework of the discrete disclination model, the stored in ISP energy $E_{ISP}$ can be calculated based on the solution for elastic field of wedge disclination in an elastic sphere [25,26]; $E_{ISP}$ can be expressed as the sum of six disclination self-energies $E_I$ and 15 energies of interaction between intersecting disclinations I and II $E_{I\text{-}II}$:

$$E_{ISP} = 6E_I + 15E_{I\text{-}II}. \quad (2)$$

Figure 2 shows a geometric scheme for calculating elastic energies $E_I$ and $E_{I\text{-}II}$.

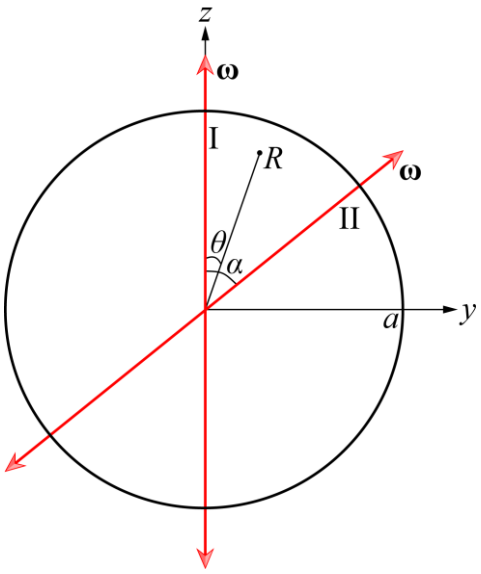


**Fig. 2.** Schematics for calculating the elastic energies of interacting wedge disclinations in a spheroid. $a$ is a sphere radius; $\theta$ and $R$ are angular and radial coordinates in the spherical coordinate system (R, $\theta$, $\varphi$), respectively

**Elastic energy of a single disclination in a spheroid**

The disclination self-energies $E_I$ can be found using general formalism of the micromechanics of defects [27]:

$$E_I = -\frac{1}{2}\int_V {}^{I}\varepsilon_{ij}^{*}\,{}^{I}\sigma_{ij}\,dV\,, \quad (3)$$

where ${}^{I}\varepsilon_{ij}^{*}$ are eigenstrains of disclination I, and ${}^{I}\sigma_{ij}$ are stresses of disclination I.

In the case of wedge disclination defined by the position of its line $x = 0$, $0 \le R \le a$ and $0 \le \theta \le \pi$ (see Fig. 2), the eigenstrain of positive disclination I, can be written as:

$${}^{I}\varepsilon_{xx}^{*} = -\omega y H[(\pi-\theta),\theta]H(a-R)\delta(x) = -\omega R\sin\theta\, H[(\pi-\theta),\theta]H[a-R]\delta(x), \quad (4)$$

where $H[\xi]$ is Heaviside function, $\delta(x)$ is Dirac delta function. Using Eqs. (3) and (4) the energy of a single disclination in a sphere can be modified as follows:

$$E_I = -\frac{1}{2}\int_V {}^{I}\varepsilon_{xx}^{*}\,{}^{I}\sigma_{xx}dV = \frac{\omega}{2}\int_0^a\int_0^\pi R^2\sin\theta\;{}^{I}\sigma_{xx}\,|_{x=0}\;dRd\theta\,, \quad (5)$$

with the known disclination stress component ${}^{I}\sigma_{xx}\,|_{x=0} = {}^{I}\sigma_{\varphi\varphi}$ [25]:

$$
{}^{\mathrm{I}}\sigma_{xx}|_{x=0} = {}^{\mathrm{I}}\sigma_{\varphi\varphi} = -\frac{G\omega}{60\pi(1-\nu)(7+5\nu)} \times
$$

$$
\times\left[75\nu(1+3\nu)\left(\frac{R}{a}\right)^2 - 4(91+53\nu) - 15(1+3\nu)(7+11\nu)\cos^2\theta\left(\frac{R}{a}\right)^2 - 30(7+5\nu)\ln\frac{R\sin\theta}{2a}\right] +
$$

$$
+\frac{G\omega}{2\pi(1-\nu)}\sum_{m=2}^{\infty}\left[\bar{A}_m(2m+1)(2m-2-2\nu-8m\nu)\left(\frac{R}{a}\right)^{2m} + 2\bar{B}_m m\left(\frac{R}{a}\right)^{2m-2}\right]P_{2m}(\cos\theta) +
$$

$$
+\frac{G\omega}{2\pi(1-\nu)}\sum_{m=2}^{\infty}\left[\bar{A}_m(2m+5-4\nu)\left(\frac{R}{a}\right)^{2m} + \bar{B}_m\left(\frac{R}{a}\right)^{2m-2}\right]P_{2m}^{1}(\cos\theta)\cot\theta\,, \qquad (6)
$$

for $m \geq 2$ $\bar{A}_m = \dfrac{(\bar{\sigma}_m - 2m\bar{\tau}_m)}{2[1+\nu+2m(1+2m+2\nu)]}$;

$$
\bar{B}_m = -\frac{(2\nu-1+4m(1+m))\bar{\sigma}_m + 2(1+\nu-4m^3+m(3+2\nu))\bar{\tau}_m}{2(2m-1)[1+\nu+2m(1+2m+2\nu)]};
$$

$$
\bar{\sigma}_m = \frac{(-2m^2\nu - m\nu + \nu + 1)(4m+1)}{(m-1)m(2m+1)(2m+3)};
$$

$$
\bar{\tau}_m = \frac{(1-2\nu)(4m+1)}{2(m-1)m(2m+1)(2m+3)},
$$

where $P_{2m}(\cos\theta)$ are Legendre polynomials, $P_{2m}^{1}(\cos\theta)$ are associated Legendre polynomials; $G$ is shear modulus; $\nu$ is Poisson's ratio.

After integrating Eq. (5), the expression for the stored (elastic energy) of a single wedge disclination in a spheroid $E_{\mathrm{I}}$ acquires the final form:

$$
E_{\mathrm{I}} = \frac{G\omega^2 a^3}{\pi(1-\nu)}\left[\frac{1}{12} - \frac{\nu(1+3\nu)}{15(7+5\nu)}\right.
$$

$$
\left. -\sum_{m=2}^{\infty}\frac{(1+4m)(32m^4\nu^2 - 8m^3(\nu^2-7\nu+1) - 4m^2(1-\nu) + 2m(11\nu^2-7\nu-9) - (1+\nu)(5-4\nu))}{4(m-1)m(2m-1)(3+8m+4m^2)^2(1+\nu+2m+4m^2+2m\nu)}\right], \qquad (7)
$$

that leads to the specific energy per unit volume of the sphere $w_1$:

$$
w_{\mathrm{I}} = \frac{3}{4}\frac{E_{\mathrm{I}}}{\pi a^3} = \frac{G\omega^2}{\pi^2(1-\nu)}\left[\frac{1}{16} - \frac{\nu(1+3\nu)}{20(7+5\nu)}\right.
$$

$$
\left. -\frac{3}{4}\sum_{m=2}^{\infty}\frac{(1+4m)(32m^4\nu^2 - 8m^3(\nu^2-7\nu+1) - 4m^2(1-\nu) + 2m(11\nu^2-7\nu-9) - (1+\nu)(5-4\nu))}{4(m-1)m(2m-1)(3+8m+4m^2)^2(1+\nu+2m+4m^2+2m\nu)}\right]. \qquad (8)
$$

Figure 3 presents the specific energy $w_1$ as a function of Poisson's ratio $\nu$. For comparison, the same Fig. 3 shows the disclination energy per unit volume of a long cylinder of radius $a$ [28]:

$$
w_{\mathrm{Icyl}} = \frac{E_{\mathrm{Icyl}}}{(\pi a^2)} = \frac{G\omega^2}{16\pi^2(1-\nu)}\,. \qquad (9)
$$

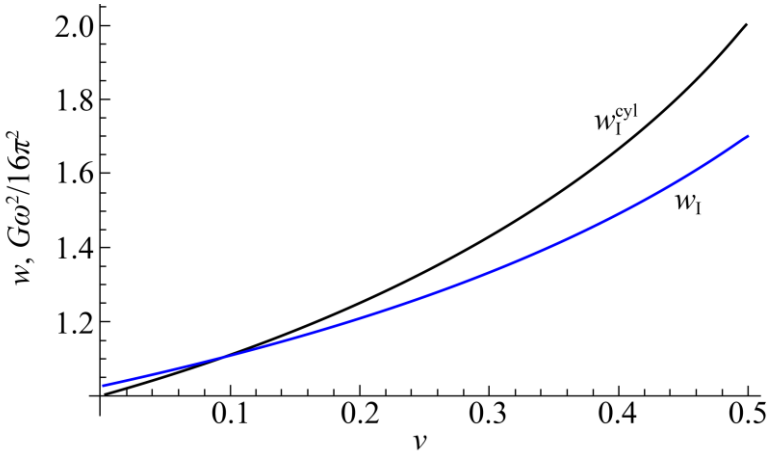


**Fig. 3.** Dependences of the elastic energy of a single wedge disclination per unit volume $w$ on the Poisson's ratio $\nu$ in a sphere and a cylinder

It is worth to note that the graphs in Fig. 3 are identical to those first given in Ref. [26], where the formula for disclination energy in a spheroid had a different from Eq. (8) form (apparently, the terms of the series were grouped in another way than in the present work).

**Interaction energy of intersecting wedge disclinations in a spheroid**

The interaction energy of intersecting disclinations in a sphere $E_{\text{I-II}}$ can also be found using general formulas of micromechanics of defects [27]:

$$E_{\text{I-II}} = -\int_V {}^{\text{I}}\varepsilon_{xx}^{*}\,{}^{\text{II}}\sigma_{xx}\,dV = \omega\int_0^a\int_0^\pi R^2\sin\theta\;{}^{\text{II}}\sigma_{xx}\,|_{x=0}\;dRd\theta\,, \tag{10}$$

where ${}^{\text{I}}\varepsilon_{ij}^{*}$ are eigenstrains of disclination I, and ${}^{\text{II}}\sigma_{ij}$ are stresses of disclination II.

Independence of the disclination elastic fields on the angle $\varphi$ in the coordinate system associated with the disclination axis, see Eq. (6), allows one to make the transition from ${}^{\text{II}}\sigma_{xx}\,|_{x=0}$ to ${}^{\text{II}}\sigma_{\varphi\varphi}$ in Eq. (10), and also write down the following relation:

$${}^{\text{II}}\sigma_{xx}\,|_{x=0} = {}^{\text{I}}\sigma_{xx}\,|_{\substack{x=0,\\ \theta\to\theta-\alpha}} \tag{11}$$

Considering Eq. (11), Eq. (10) is reduced to the following form:

$$E_{\text{I-II}} = \omega\int_0^a\int_0^\pi R^2\sin\theta\;{}^{\text{I}}\sigma_{\varphi\varphi}(\theta-\alpha)dRd\theta = \omega\int_0^a\int_{-\alpha}^{\pi-\alpha} R^2\sin(\theta'+\alpha)\;{}^{\text{I}}\sigma_{\varphi\varphi}(\theta')dRd\theta'\,. \tag{12}$$

In Eq. (12), it is necessary to account for the following: dependence ${}^{\text{I}}\sigma_{\varphi\varphi}$ on the angle $\theta$ or $\theta'$ assumes that $0 \le \theta \le \pi$. Therefore, the integration over the variable $\varphi$ in Eq. (12) should be performed by dividing the integration interval $(-\alpha, \pi-\alpha)$ into $(-\alpha, 0)$ and $(0, \pi-\alpha)$. Note that the integration over a variable $R$ gives an analytical result, and then the integration over the angle can be done numerically. In addition, it is necessary to consider the fact that for the interval $(-\alpha, 0)$, the eigenstrain of the disclination (and the elastic field) changes sign to the opposite.

Figure 4 shows the dependence of the energy of intersecting disclinations in a spheroid $E_{\text{I-II}}$ on the flat angle between disclinations $\alpha$. The five-pointed stars show calculated values, and the solid curve is the envelope.

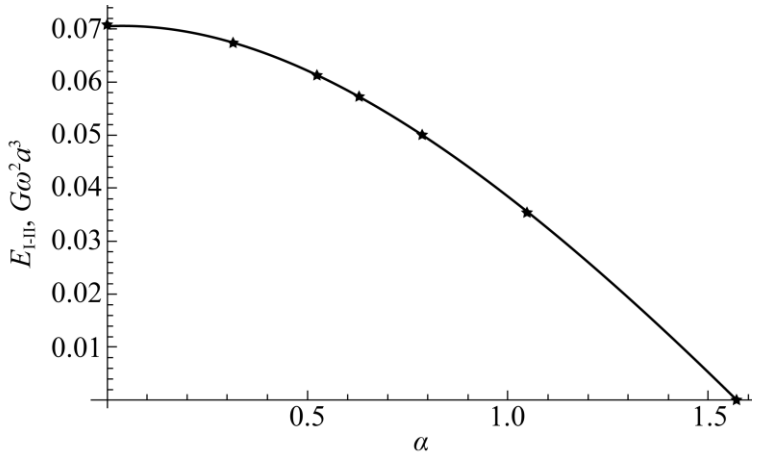


**Fig. 4.** Dependence of the energy of intersecting wedge disclinations in a spheroid $E_{\text{I-II}}$ on the flat angle $\alpha$ between them

**Results and Discussion**

It is obvious that in the case of coincidence of two interacting disclinations ($\alpha = 0$ or $\alpha = \pi$), the interaction energy between two dislocations is equal to twice the elastic energy of a single disclination: $E_{\text{I-II}} = 2E_{\text{I}}$, and the total energy of such a system is $4E_{\text{I}}$. This corresponds to the single disclination energy $E_{\text{I}}$ with strength $2\omega$ ($\omega \to 2\omega$ in Eq. (7)). At mutually perpendicular position of disclinations ($\alpha = \pi/2$), the integral interaction energy between two dislocations $E_{\text{I-II}}$ is zero.

Consider all the results of the analytical and numerical calculations, the stored in the ISP elastic energy $E_{\text{ISP}}$ defined within the framework of discrete disclination model can be calculated by exploring Eq. (2) ($\alpha = 63.435°$, $\omega \approx 7.333°$, $\nu = 0.3$):

$$E_{\text{IPP}} \approx 0.687G\omega^2a^3 \approx 0.0113Ga^3. \quad (13)$$

For comparison, let us find the value of ISP energy in the distributed disclination model (Marx-Ioffe model), in which six intersecting disclinations are replaced by continuously distributed conical stereo disclinations with total strength $\chi = 3\omega/2\pi \approx 0.06$ [17]:

$$E_{\text{IPP}}^{\chi} = \frac{8\pi(1+\nu)G\chi^2a^3}{27(1-\nu)} = \left.\frac{2(1+\nu)G\omega^2a^3}{3\pi(1-\nu)}\right|_{\nu=0.3} \approx 0.394G\omega^2a^3\Big|_{\omega\approx 7.333°} \approx 0.00646Ga^3. \quad (14)$$

For the same radius of spheroid, the distributed disclination model gives a lower value of ISP energy compared to those found with the discrete disclination model, at least for the Poisson's ratio $\nu = 0.3$, the energy values differ by 1.7 times: $E_{\text{IPP}} / E_{\text{IPP}}^{\chi} \approx 1.7$. Table 1 shows the ratio of the stored in ISP energies calculated within the framework of two models (discrete and distributed ones) for several values of Poisson's ratio $\nu$.

**Table 1.** Icosahedral small particle energy values found within discrete ($E_{\text{ISP}}$) and distributed ($E_{\text{IPP}}^{\chi}$) disclination models for several values of Poisson's ratio

| Poison's ratio $\nu$ | $E_{\text{ISP}}$, $G\omega^2a^3$ | $E_{\text{ISP}}^{\chi}$, $G\omega^2a^3$ | $E_{\text{ISP}} / E_{\text{ISP}}^{\chi}$ |
|---|---|---|---|
| 0 | 0.528 | 0.212 | 2.5 |
| 0.1 | 0.576 | 0.259 | 2.2 |
| 0.2 | 0.626 | 0.318 | 2.0 |
| 0.3 | 0.687 | 0.394 | 1.7 |
| 0.4 | 0.785 | 0.495 | 1.6 |
| 0.5 | 0.882 | 0.637 | 1.4 |

As can be seen from Tab. 1, for any positive values of Poison's ratio $\nu$, ISP energy in discrete disclination model is larger than in distributed disclination model: $E_{\text{IPP}} > E_{\text{IPP}}^{\chi}$, and

with a decrease in the Poisson's ratio $\nu$ of the ISP material, the discrepancy in ISP energy within discrete and distributed models becomes larger.

## Conclusions

In this work, we have presented the discrete disclination model of icosahedral small particles (ISPs). The discrete disclination model considers ISP as an elastic spheroid with six positive wedge disclinations passing through its center in opposite to the distributed disclination model based on conical stereo disclinations continuously distributed over spheroid volume. In order to calculate the stored (elastic) in ISP energy, the pair interaction energy of disclinations in a spheroid has been calculated for the first time as a function of the plane angle between wedge disclinations. It has been shown that for disclinations located strictly opposite each other, the energy of their interaction is equal to twice the elastic energy of the single disclination in the sphere. On the other hand, for disclinations located at right angles to each other, the interaction energy has zero value.

We have also analyzed the influence of Poison's ratio on the energy of ISP found within both discrete and distributed disclination models. It has been established that for any positive values of Poisson's ratio of ISP material, the stored energy calculated within the discrete disclination model demonstrates larger values than those calculated within the distributed disclination model. The differences are stronger, the smaller the value of Poisson's ratio.

Summarizing the findings, the discrete disclination model proposed opens the possibility to the strict analysis of icosahedral small particles.

## References

1. Shechtman D, Blech I, Gratias D, Cahn JW. Metallic phase with long-range orientational order and no translational symmetry. *Physical Review Letters*. 1984;53(20): 1951–1953.
2. Cahn JW, Shechtman D, Gratias D. Indexing of icosahedral quasiperiodic crystals. *Journal of Materials Research*. 1986;1(1): 13–26.
3. Steurer W. Twenty years of structure research on quasicrystals. Part I. Pentagonal, octagonal, decagonal and dodecagonal quasicrystals. *Zeitschrift für Kristallographie - Crystalline Materials*. 2004;219(7): 391–446.
4. Ino S. Epitaxial growth of metals on rocksalt faces cleaved in vacuum. II. Orientation and structure of gold particles formed in ultrahigh vacuum. *Journal of the Physical Society of Japan*. 1966;21(2): 346–362.
5. Galligan JM. Fivefold symmetry and disclinations. *Scripta Metallurgica*. 1972;6(2): 161–163.
6. Marks LD, Smith DJ. High resolution studies of small particles of gold and silver. *Journal of Crystal Growth*. 1981;54(3): 425–32.
7. Gryaznov VG, Heydenreich J, Kaprelov AM, Nepijko SA, Romanov AE, Urban J. Pentagonal Symmetry and Disclinations in Small Particles. *Crystal Research and Technology*. 1999;34(9): 1091–119.
8. Romanov AE, Kolesnikova AL. Elasticity boundary-value problems for straight wedge disclinations. A review on methods and results. *Reviews on Advanced Materials and Technologies*. 2021;3(1): 55–95.
9. Wu J, Qi L, You H, Gross A, Li J, Yang H. Icosahedral platinum alloy nanocrystals with enhanced electrocatalytic activities. *Journal of the American Chemical Society*. 2012;134(29): 11880–11883.
10. Ji G, Ji A, Lu N, Cao Z. Formation and morphology evolution of icosahedral and decahedral silver crystallites from vapor deposition in view of symmetry misfit. *Journal of Crystal Growth*. 2019;518: 89–94.
11. Liu M, Lyu Z, Zhang Y, Chen R, Xie M, Xia Y. Twin-directed deposition of Pt on Pd icosahedral nanocrystals for catalysts with Enhanced activity and durability toward oxygen reduction. *Nano Letters*. 2021;21(5): 2248–2254.
12. Sharma M, Pudasaini PR, Ruiz-Zepeda F, Vinogradova E, Ayon AA. Plasmonic effects of

Au/Ag bimetallic multispiked nanoparticles for photovoltaic applications. *ACS Applied Materials & Interfaces*. 2014;6(17): 15472–15479.
13. Fontana J, Dressick WJ, Phelps J, Johnson JE, Rendell RW, Sampson T et al. Virus-templated plasmonic nanoclusters with icosahedral symmetry via directed self-assembly. *Small*. 2014;10(15): 3058–3063.
14. Gutkin MY. Elastic behavior of defects in nanomaterials I. Models for infinite and semi-infinite media. *Reviews on Advanced Materials Science*. 2006;13(2): 125–161.
15. Ovid'ko IA, Sheinerman AG. Plastic deformation and fracture processes in metallic and ceramic nanomaterials with bimodal structures. *Reviews on Advanced Materials Science*. 2007;16: 1–9.
16. Romanov AE, Kolesnikova AL. Micromechanics of defects in functional materials. *Acta Mechanica*. 2021;232(5): 1901–1915.
17. Howie A, Marks LD. Elastic strains and the energy balance for multiply twinned particles. *Philosophical Magazine A*. 1984;49(1): 95–109.
18. Dorogin LM, Vlassov S, Kolesnikova AL, Kink I, Lõhmus R, Romanov AE. Crystal mismatched layers in pentagonal nanorods and nanoparticles. *Physica Status Solidi (B)*. 2010;247(2): 288–298.
19. Lu L, Wang J, Zheng H, Zhao D, Wang R, Gui J. Spontaneous formation of filamentary Cd whiskers and degradation of CdMgYb icosahedral quasicrystal under ambient conditions. *Journal of Materials Research*. 2012;27(14): 1895–1904.
20. Vikarchuk AA, Dorogov M V. Features of the evolution of the structure and morphology of the surface of icosahedral copper particles in the annealing process. *JETP Letters*. 2013;97(10): 594–598.
21. Abramova AN, Dorogov MV, Vlassov S, Kink I, Dorogin LM, Lohmus R et al. Nanowhisker of copper oxide: fabrication technique, structural features and mechanical properties. *Materials Physics and Mechanics*. 2014;19: 88–95.
22. Romanov AE, Vikarchuk AA, Kolesnikova AL, Dorogin LM, Kink I, Aifantis EC. Structural transformations in nano- and microobjects triggered by disclinations. *Journal of Materials Research*. 2012;27(3): 545–551.
23. Grünbaum B. Regular polyhedra–old and new. *Aequationes Mathematicae*. 1977;16(1–2): 1–20.
24. Hargittai I. Fivefold symmetry. Budapest: World Scientific Publishing; 1992.
25. Kolesnikova AL, Gutkin MY, Proskura AV, Morozov NF, Romanov AE. Elastic fields of straight wedge disclinations axially piercing bodies with spherical free surfaces. *International Journal of Solids and Structures*. 2016;99: 82–96.
26. Polonsky IA, Romanov AE, Gryaznov VG, Kaprelov AM. Disclination in an elastic sphere. *Philosophical Magazine A*. 1991;64(2): 281–287.
27. Mura T, Barnett DM. Micromechanics of Defects in Solids. *Journal of Applied Mechanics*. 1983;50(2): 477–477.
28. Romanov AE, Vladimirov VI. Disclinations in crystalline solids. In: *Dislocations in solids*. Amsterdam: North-Holland; 1992.

## THE AUTHORS

**A.L. Kolesnikova**
e-mail: anna.kolesnikova.physics@gmail.com

**M.V. Dorogov**
e-mail: mvdorogov@itmo.ru

**S.A. Krasnitckii**
e-mail: Krasnitsky@inbox.ru

**A.M. Smirnov**
e-mail: andrei.smirnov@niuitmo.ru

**A.E. Romanov**
alexey.romanov@niuitmo.ru